Measurement of the cross-section ratio $\sigma_{\psi(2S)}/\sigma_{J/\psi(1S)}$ in exclusive photoproduction at HERA

Grzegorz Grzelak
(on behalf of the ZEUS collaboration)

Faculty of Physics
University of Warsaw

42nd International Conference on High Energy Physics, ICHEP-2024, 17 - 24 July 2024, Prague

HERA and ZEUS: 1992 – 2007, DESY, Hamburg

HERA: world's first and only $e^{\pm}p$ collider, $\mathbf{E_e = 27.5}$ **GeV**, $\mathbf{E_p = 920}$ **GeV** ($\sqrt{s} = 318$ GeV)

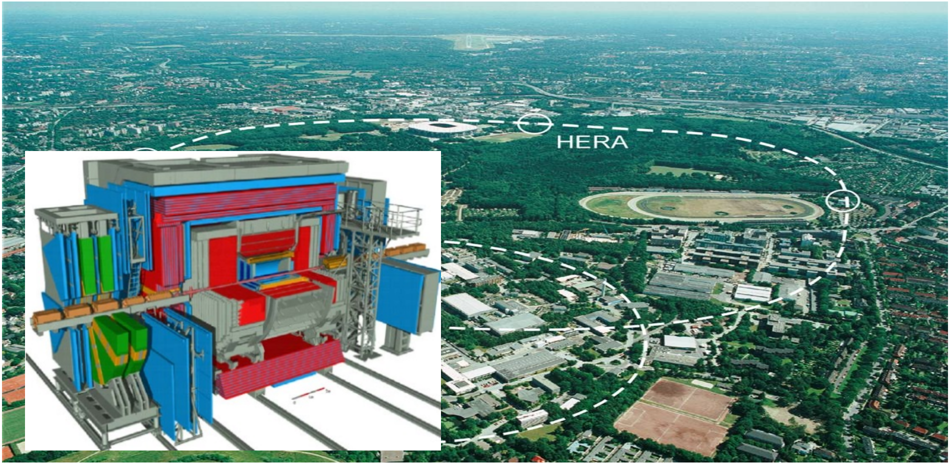

ZEUS: multipurpose, hermetic detector (MVD, CTD, CAL, F/B/RMUON, BAC, ...)
Total luminosity: $\int \mathcal{L} \sim \mathbf{500\ pb^{-1}}$ collected during HERA I + II running periods

Production of Vector Mesons in Exclusive Diffraction in *ep* Scattering

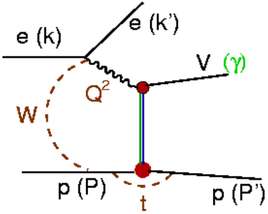

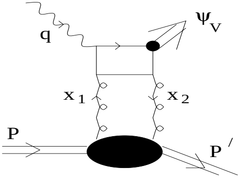

Exclusive process: proton stays intact

Proton dissociation also possible → background

Kinematics: $\mathbf{M_V^2}, \mathbf{Q^2}, \mathbf{W}, |\mathbf{t}|$

M_V^2 - vector meson mass squared

Q^2 $(= -q^2 = -(k - k')^2)$ - the photon virtuality (emitted by the incoming electron):

- $Q^2 \approx 0$ GeV^2 PHP (*Photoproduction*)
- larger Q^2 for DIS (*Deep Inelastic Scattering*)

$W = (q + P)^2$ - invariant mass of the γp system

$W \approx \sqrt{2E_P(E - p_Z)_V}$

$|t|$ - 4-momentum transfer at the proton vertex

$t = (P - P')^2$

$t \approx -p_{T,V}^2$

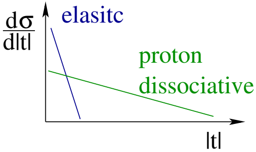

pQCD: M_V^2 and Q^2 - set the scale at which the W and $|t|$ are probed

Process sensitive to the **gluon density** in the proton

Cross section ratio $\psi(2S)/J/\psi(1S)$

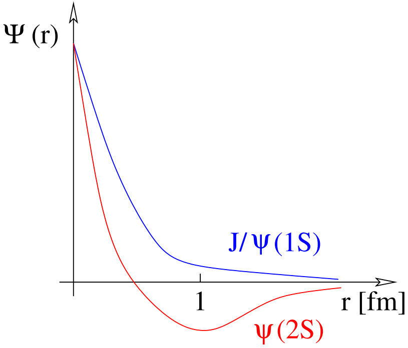

$$\text{Ratio } R = \frac{\sigma_{\gamma p \to \psi(2S)p}}{\sigma_{\gamma p \to J/\psi(1S)p}}$$

- sensitive to radial wave function of charmonium
- provides insight into the dynamics of the hard process

- $J/\psi(1S)$ and $\psi(2S)$ have the same quark composition but distinctive wave functions
- $\psi(2S)$ has a node at ≈ 0.4 fm
- $\langle r^2_{\psi(2S)} \rangle \approx 2 \langle r^2_{J/\psi(1S)} \rangle$
- pQCD models predict $R \sim 0.17$ in PHP and rise of R with Q^2 in DIS
- $\psi(2S)$ **cross section is expected to be suppressed w.r.t. the** J/ψ **production**
- (Both Vector Mesons masses are much smaller then the γp center-of-mass energy)

- **Signal MC:** DIFFVM (VM production in *ep* scattering)

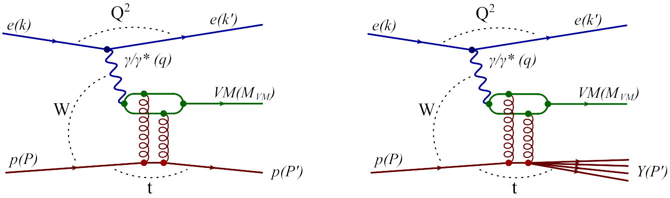

- **Background MC:** GRAPE (Bethe-Heitler continuum $\mu^+\mu^-$)

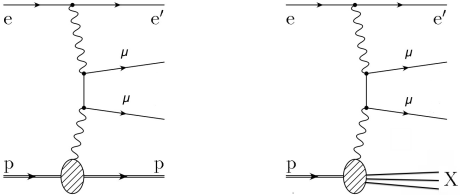

- **HERA II DATA:** $\mathcal{L} = 373$ pb^{-1} (2003 - 2007)
- **Investigated decay channels:**
  - $\psi(2S) \to J/\psi + \pi^+\pi^-$, $\psi(2S) \to \mu^+\mu^-$, $J/\psi(1S) \to \mu^+\mu^-$
- exclusive (elastic) photoproduction sample

Example of Final State Topology for $ep \to J/\psi p$, $J/\psi \to \mu^+\mu^-$

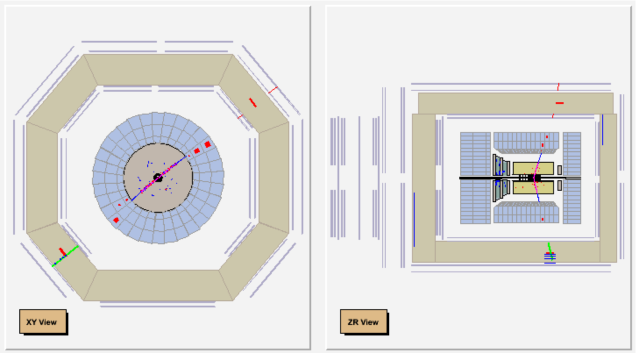

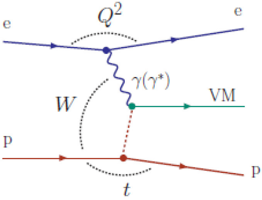

Exclusive process, reaction mediated by exchange of colorless object;
proton stays intact.

J/ψ and $\psi(2S)$ are detected in the 2- or 4-prong final states ($\mu^+\mu^-$ or $\mu^+\mu^-\pi^+\pi^-$)
very clean final state topology:

Photoproduction ($Q^2 < 1$ GeV^2): two or four charged particles and nothing else
$\Longrightarrow$ **experimental challenge: triggering on soft muons**
(Electroproduction ($Q^2 > 1$ GeV^2): scattered electron also visible in the detector)

NOTE THE OPENING ANGLE OF THE DECAY PRODUCTS

Event Selection: 2-prongs sample: J/ψ, $\psi(2S) \to \mu^+\mu^-$

- Exclusive Muon Triggers (F/B/R/MUON or BAC)
- Tracking and Vertex
  - $N_{track} = 2$, oppositely charged tracks matched to the primary vertex ($\eta \in (-1.9, 1.9)$)
  - **both tracks identified as a muon in CAL, at least one in F/B/RMUON or BAC**
  - $p_T > 1.0$ GeV of each track
  - anti-COSMIC cuts (CAL timing, acolinearity: $\cos(\mu^+, \mu^-) < -0.985$)
- Elasticity/Exclusivity and Photoproduction cuts (on CAL Energy)
  - no scattered electron found in CAL
  - $E_{\mathrm{clu}} < 0.5$ GeV for clusters not matched to muons (or pions)
    (corresponds to an effective cut on $Q^2 < 1$ GeV^2)
  - $E(\theta < 0.12 rad) < 1$ GeV
    the sum of the energy in the FCAL cone around the beam-pipe;
    to suppress proton-dissociative events, $ep \to e + VM + Y$
    (corresponds to a requirement for $M_Y \lesssim 5$ GeV)
- Kinematic range (analysis phase space):
  - $30 < W < 180$ GeV
  - $|t| < 1.0$ GeV^2
  - $Q^2 < 1$ GeV^2 (median $Q^2 \approx 3 \times 10^{-5}$ GeV^2)

- (for 4-prongs selection see backup plots)

- **Signal Extraction, Mass spectra**

$M(\mu^+\mu^-)$

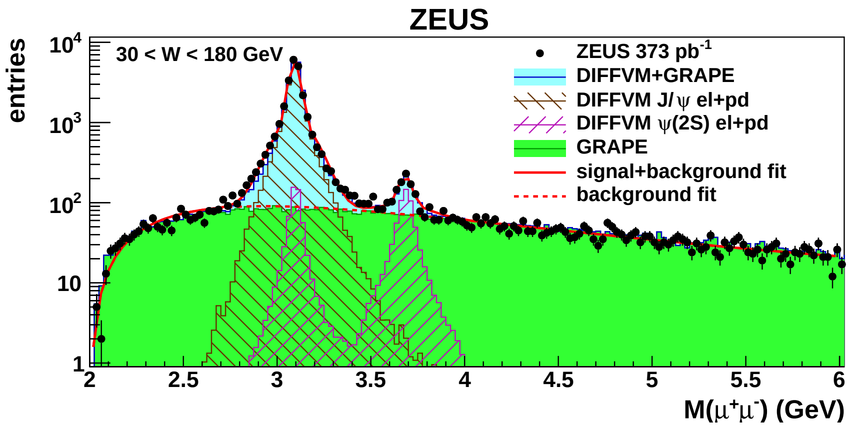

- **full phase space:** $30 < W < 180$ GeV, $|t| < 1.0$ GeV^2
- events yield: $\sim 23\,000$ J/ψ and ~ 700 $\psi(2S)$ (from double Gaussian fit)
- resonant background under J/ψ peak

$M(\mu^+\mu^-)$

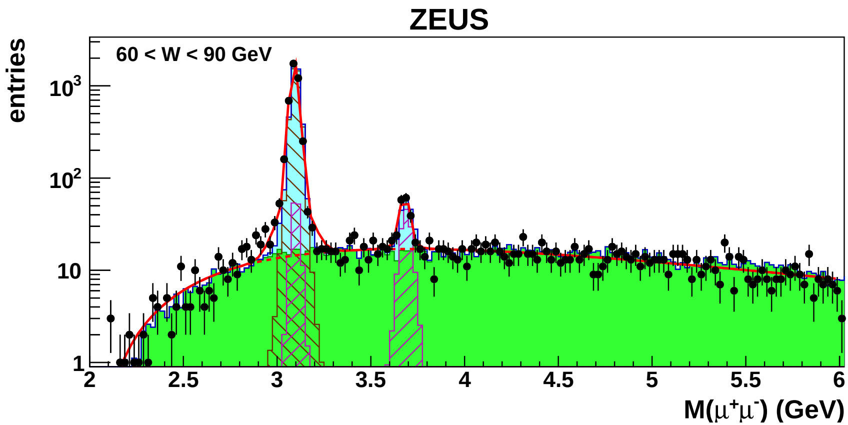

- **W2 bin:** $60 < W < 90$ GeV, $|t| < 1.0$ GeV^2
- central rapidity region, long tracks, mass resolution: $\sigma_M(\mu\mu) \sim 22$ MeV

2-prongs: dimuon mass spectra

$M(\mu^+\mu^-)$

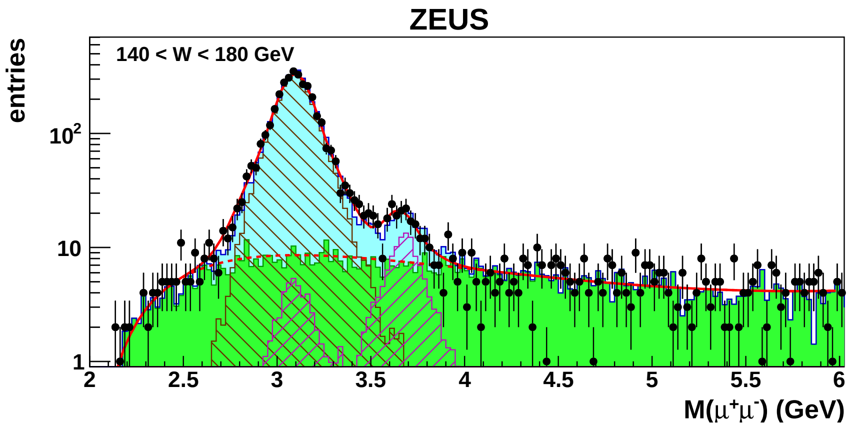

- **W5 bin:** $140 < W < 180$ GeV, $|t| < 1.0$ GeV^2
- high W, backward short tracks, mass resolution: $\sigma_M(\mu\mu) \sim 73$ MeV

2-prongs: dimuon mass spectra

$M(\mu^+\mu^-)$

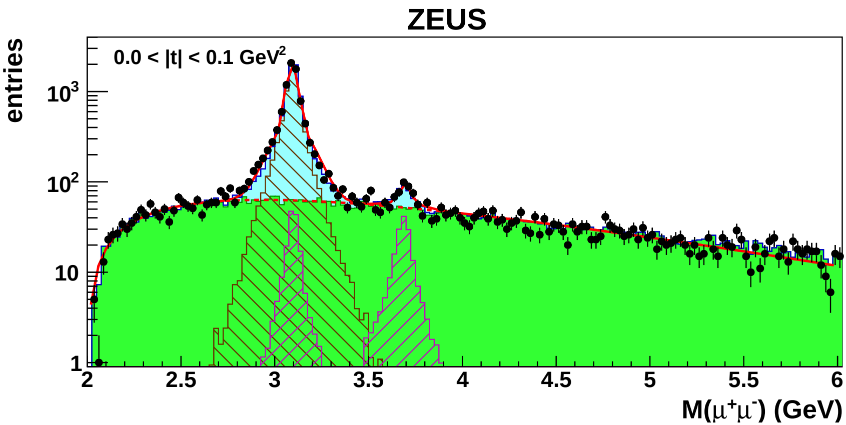

- **t1 bin:** $30 < W < 180$ GeV, $|t| < 0.1$ GeV^2
- low $|t|$, dominated by Bethe-Heitler continuum $\mu^+\mu^-$ background

2-prongs: dimuon mass spectra

$M(\mu^+\mu^-)$

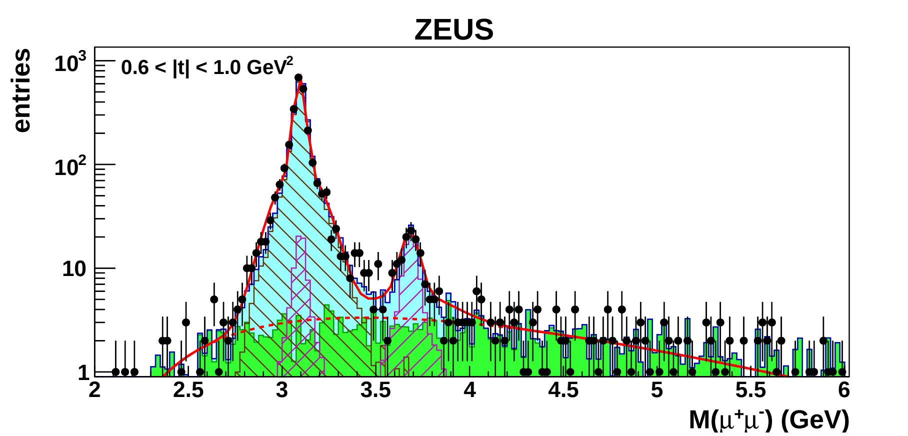

- **t5 bin:** $30 < W < 180$ GeV, $0.6 < |t| < 1.0$ GeV^2
- higher $|t|$, small Bethe-Heitler continuum $\mu^+\mu^-$ contribution
- **BUT: high contamination proton dissociative events** $\rightarrow$ t spectra

4-prongs: mass spectra

$M(\mu^+\mu^-\pi^+\pi^-)$

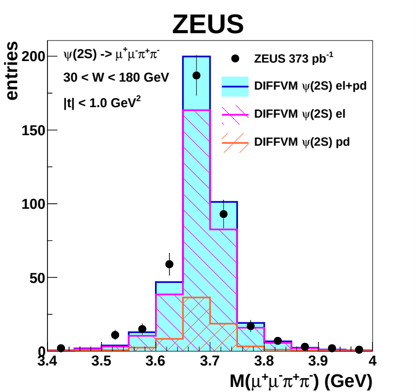

$M(\mu^+\mu^-\pi^+\pi^-) - M(\mu^+\mu^-)$

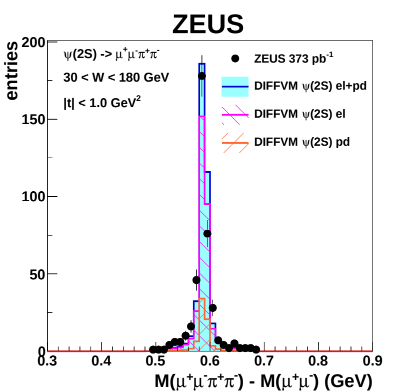

- events yield: $\sim 400\ \psi(2S)$ (background free)
- better resolution on mass difference $\rightarrow$ cascade decay of $\psi(2S)$
- proton dissociative fraction: $f_{p.diss} = 0.16 \pm 0.01$ from t-spectra fit

- **W and $|t|$ distributions: 2-prongs**

2-prongs: W and $|t|$ distributions: J/ψ mass window

W: $2.8 < M(\mu^+\mu^-) < 3.4$ GeV

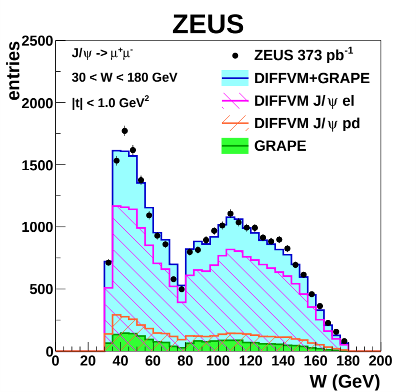

$|t|$: $2.8 < M(\mu^+\mu^-) < 3.4$ GeV

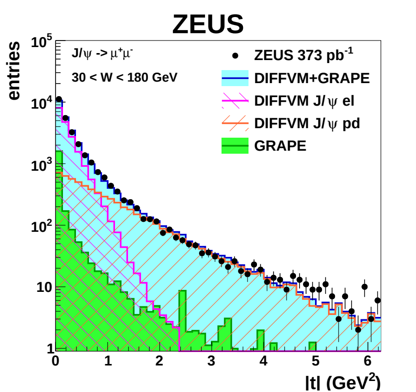

- dip in W distribution due to the anti-COSMIC cut: $\cos(\mu^+, \mu^-) < -0.985$
- proton dissociation dominates for $|t| > 1.0$ GeV^2
- proton dissociative fraction: $f_{p.diss} = 0.17 \pm 0.01$ ($|t| < 1.0$ GeV^2) from t-spectra fit

2-prongs: W and $|t|$ distributions: $\psi(2S)$ mass window

W: $3.4 < M(\mu^+\mu^-) < 4.0$ GeV

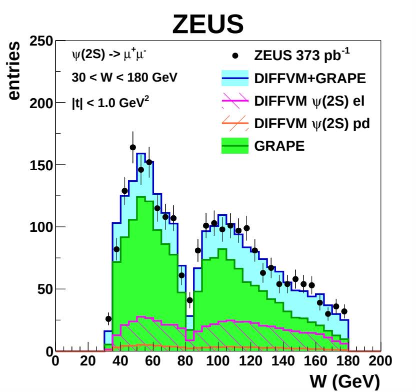

$|t|$: $3.4 < M(\mu^+\mu^-) < 4.0$ GeV

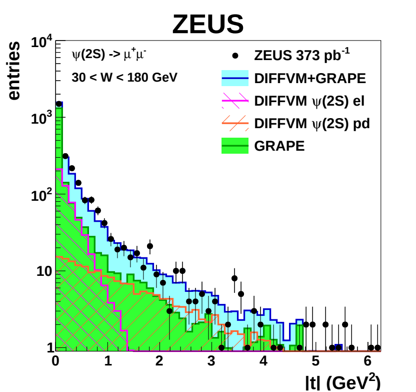

- dip in W distribution due to the anti-COSMIC cut: $\cos(\mu^+, \mu^-) < -0.985$
- proton dissociation dominates for $|t| > 1.0$ GeV^2
- channel dominated by Bethe-Heitler continuum $\mu^+\mu^-$ background

- **Cross section ratio**

Cross section ratio $R = \frac{\sigma(\psi(2S))}{\sigma(J/\psi(1S))}$, full kinematic range

$30 < W < 180$ GeV, $|t| < 1.0$ GeV^2, $Q^2 < 1.0$ GeV^2

$\psi(2S)$ decay mode	$R = \frac{\sigma(\psi(2S))}{\sigma(J/\psi(1S))}$
$\mu^+\mu^-$	0.154 ± 0.012
$J/\psi(\rightarrow \mu^+\mu^-)\pi^+\pi^-$	0.125 ± 0.019
combined	$0.146 \pm 0.010^{+0.016}_{-0.020}$

- $R_{J/\psi\pi\pi} = \frac{N_{\psi(2S)}}{N_{J/\psi(1S)}} \cdot \frac{Acc_{J/\psi(1S)\rightarrow\mu^+\mu^-}}{Acc_{\psi(2S)\rightarrow J/\psi\pi^+\pi^-}} \cdot \frac{1}{BR_{\psi(2S)\rightarrow J/\psi\pi^+\pi^-}} \cdot \frac{1-f_{pdiss}^{\psi(2S)}}{1-f_{pdiss}^{J/\psi(1S)}}$
- $R_{\mu\mu} = \frac{N_{\psi(2S)}}{N_{J/\psi(1S)}} \cdot \frac{Acc_{J/\psi(1S)\rightarrow\mu^+\mu^-}}{Acc_{\psi(2S)\rightarrow\mu^+\mu^-}} \cdot \frac{BR_{J/\psi(1S)\rightarrow\mu^+\mu^-}}{BR_{\psi(2S)\rightarrow\mu^+\mu^-}} \cdot \frac{1-f_{pdiss}^{\psi(2S)}}{1-f_{pdiss}^{J/\psi(1S)}}$
- $Acc_i = \frac{N_i^{reco}}{N_i^{true}}$, $f_{p.diss}^i$ - fraction of proton dissociative events
- $BR(\psi(2S) \rightarrow J/\psi\pi^+\pi^-) = (34.68 \pm 0.3)\%$, $BR(\psi(2S) \rightarrow \mu^+\mu^-) = (0.80 \pm 0.06)\%$,
  $BR(J/\psi \rightarrow \mu^+\mu^-) = (5.961 \pm 0.033)\%$, $BR(\psi(2S) \rightarrow \mu^+\mu^-\pi^+\pi^-) = (2.07 \pm 0.02)\%$ (PDG 2020)
- both channels have similar precision and provide consistent results

cross section ratio $R = \sigma_{\psi(2S)}/\sigma_{J/\psi(1S)}$: 2- and 4-prongs comparison

R vs. W

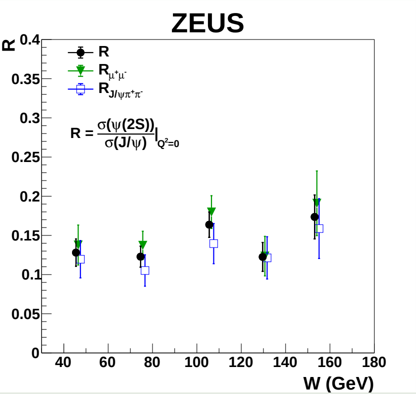

R vs. $|t|$

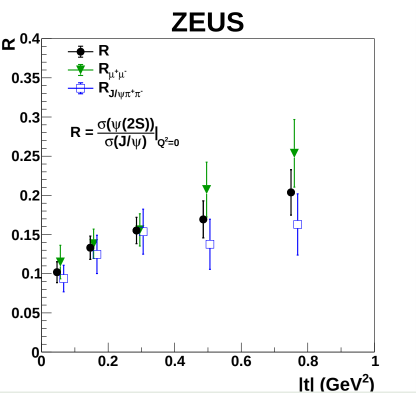

- $R_{\mu\mu}$ (2-prongs channel), $R_{J/\psi\pi\pi}$ (4-prongs channel) and combined R (full dots)
- statistical errors only
- **good agreement between two channels**

cross section ratio $R = \sigma_{\psi(2S)}/\sigma_{J/\psi(1S)}$: Final Results

R vs. W

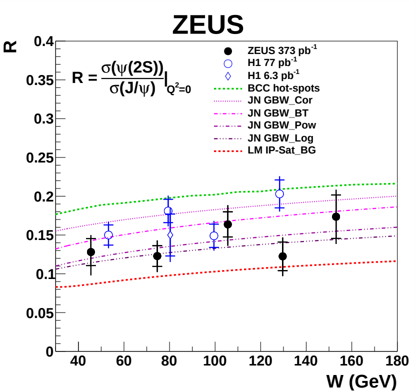

R vs. $|t|$

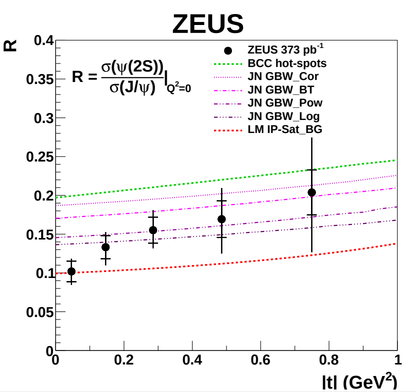

- for R vs. W ZEUS (full dots) and H1 (open markers) results are compared
- **no W dependence observed, moderate increase with $|t|$**
- good agreement between data and theoretical models (see next page)
- errors at high-$|t|$ points dominated by systematics ($\rightarrow$ proton dissociative fraction)

R vs. Q^2

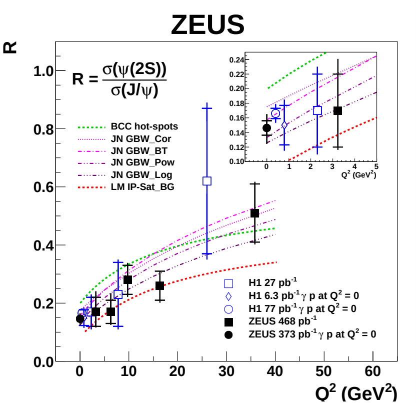

theoretical models:

- Bendova, Cepila and Contreras (BCC hot-spots):
  - Phys. Rev. **D 99**, 034025 (2019).
- Jan Nemchik et al. (JN):
  - Eur. Phys. J. **C 79**, 154 (2019).
  - Eur. Phys. J. **C 79**, 495 (2019).
  - Phys. Rev. **D 103**, 094027 (2021).
- Lappi and Mäntysaari (LM IP-Sat):
  - Phys. Rev. **C 83**, 065202 (2011).
  - Phys. Rev. **D 87**, 034002 (2013).
  - PoS (DIS2014), 069 (2014).

- ZEUS (full dot) and H1 (open markers) photoproduction results plotted at $Q^2 \sim 0$
- DIS results are also presented vs. Q^2: ZEUS (full squares) and H1 (open squares)
- good agreement between data and theoretical models (→ backup plots, page 30)
- **better precision of photoproduction points**

Summary

- **Cross section ratio** $\mathbf{R} = \frac{\sigma(\psi(2S))}{\sigma(J/\psi(1S))}$ in photoproduction using HERA II data was measured by ZEUS in the kinematic range: $30 < W < 180$ GeV, $|t| < 1.0$ GeV^2
- first ZEUS measurement of R in photoproduction (at $Q^2 = 0$):
  $R = 0.146 \pm 0.01(stat.)^{+0.016}_{-0.022}(syst.)$
- first HERA result for R vs. $|t|$ in photoproduction
- **moderate rise of cross section ratio as a function of** $|t|$
- **no** W **dependence observed within experimental errors**
- consistent results for 2- and 4-prongs decay channels
- comparable precision in both decay channels
- **theoretical calculations of the ratio** $\frac{\sigma(\psi(2S))}{\sigma(J/\psi(1S))}$ **for exclusive vector-meson production has been compared to the experimental data**
- → majority of the predictions are consistent with the data
- **data start to exhibit constraining power**
- for more details see: `https://doi.org/10.1007/JHEP12(2022)164`

Thank You For Your Attention

BACKUP PLOTS FOLLOWS...

- **Systematics**

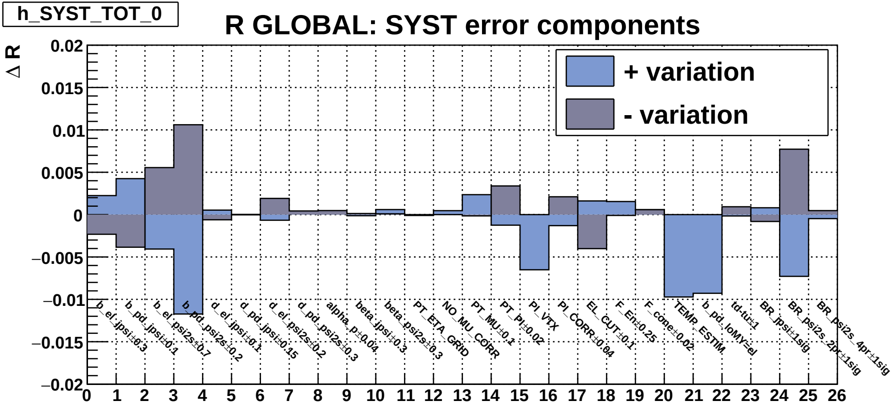

- biggest contributions from:
- b-slope variation of t-dependence (esp. for b_{pd} of $\psi(2S)$)
- event number estimator (MC templates fit instead of Gaussian fit)
- slow pions vertexing
- $BR(\psi(2S) \to \mu^+\mu^-)$

R: components of SYST. error in W and $|t|$ bins

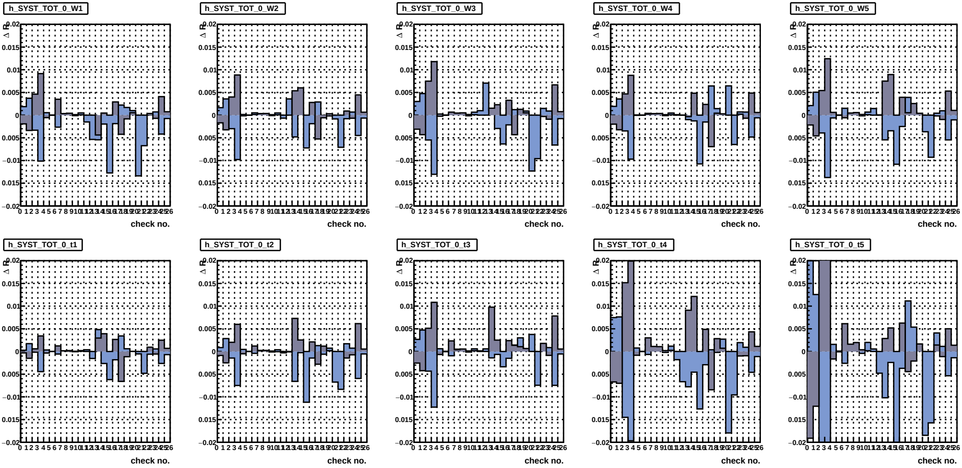

- upper row: contributions in 5 W bins
- bottom row: contributions in 5 $|t|$ bins
- bin order as on previous page

- **Theoretical Models**

Theory predictions: models (1)

- **Bendova, Cepila and Contreras (BCC hot-spots) :**
- Phys. Rev. D **99**, 034025 (2019).
- model with hot spots randomly sampled in the transverse plane bound by the size of the proton
- The slope parameter b is 4.72 GeV^{-2} and it is fixed by the combined H1 and ZEUS data from 2013 for JPsi photoproduction t-distribution.
- the same b-slope for both JPsi and Psi2s

- **Jan Nemchik (JN) et al. :**
- Eur. Phys. J. C **79**, no.6, 495 (2019).
- Eur. Phys. J. C **79**, no.2, 154 (2019).
- calculations have been performed for various combinations of quarkonium wave functions:
  - **Cor** (Cornell potential)
  - **BT** (Buchmüller-Tye)
  - **Pow** (Power-law potential)
  - **Log** (Logarithmic potential)

  and models for the dipole cross sections:
  - BGBK, **GBW** ← **used on the plots**
  - for each combinations calculations are performed with and w/o skewness in the gluon density
- the same b-slope parameters for both quarkonium states

Theory predictions: models (3)

- **Lappi and Mäntysaari (LM IP-Sat):**
- the BFKL evolution plus the IP-Sat model to predict vector-meson production in ep and electronion collisions in the dipole picture
- 2S parameters from arXiv:1406.2877 (PoS DIS2014 (2014) 069)
- 1S parameters from hep-ph/0606272 (Phys.Rev. **D74** (2006) 074016)
- Calculation described in (Phys.Rev. **C83** (2011) 065202)
- **IP-Sat** dipole from fit (Phys.Rev. **D87** (2013) no.3, 034002)
- Wave function: Boosted Gaussian (**BG**), $Q^2 = 0$ GeV^2
- Skewedness and real part corrections included

- predictions of all models were calculated within the phase space of this analysis:
  - $30 < W < 180$ GeV
  - $|t| < 1.0$ GeV^2
  - $Q^2 \sim 0$ (photoproduction points)

- **Signal extraction, cuts, control plots, ...**

2-prongs: Signal extraction: fit parameterization

- Double Gaussian shape: $G(x)$ or $g(x) = N \cdot \Delta \cdot \frac{1}{\sqrt{2\pi}\sigma} \exp\left(-\frac{(x-m)^2}{2\sigma^2}\right)$
  where: N – number of events, Δ – mass bin width,
  m – mean value, σ – RMS
- for J/ψ: $N_1 \cdot G_1(x) + N_2 \cdot G_2(x)$
- for ψ': $N_1' \cdot g_1(x) + N_2' \cdot g_2(x)$
- introducing: $N = N_1 + N_2,\ N' = N_1' + N_2',\ R = \frac{N'}{N}$
- with additional constrains: $m_1 = m_2,\ m_1' = m_2',$
  $\frac{\sigma_1'}{\sigma_1} = \frac{\sigma_2'}{\sigma_2} = \alpha,\ \xi = \frac{N_1}{N} = \frac{N_1'}{N'}$ **(scaling of the mass resolution)**
- final formulae:

$$F(x) = N \cdot ((\xi \cdot G_1(x) + (1-\xi) \cdot G_2(x)) + R \cdot (\xi \cdot g_1(x) + (1-\xi) \cdot g_2(x))) + BG(x)$$

- background function: $BG(x) = A \cdot (x-B)^C \cdot \exp(-D(x-B) - E(x-B)^2)$
  where A, B, C, D, E are fit parameters, B fixed $(= 2p^{\mu}_{t,min})$

Event Selection: 4-prongs sample: $\psi(2S) \to \mu^+\mu^-\pi^+\pi^-$

- (only differences w.r.t. the 2-prong channel)
- $N_{track} = 4$, (two oppositely charged pairs, sorted by p_T)
- highest momentum pair: muon candidates
  lowest momentum pair: pion candidates
- no anti-COSMIC cuts
- transverse momentum of pion candidates: $p_T^\pi > 0.12$ GeV;
- $2.8 < M(\mu^+\mu^-) < 3.4$ GeV (J/ψ window)
- $M(\mu^+\mu^-\pi^+\pi^-) - M(\mu^+\mu^-)$ in $(0.5 - 0.7)$ GeV window
  (cascade decay of $\psi(2S)$)

- QED di-muons (like $\gamma^*\gamma^* \to \mu^+\mu^-$) from the Bethe-Heitler process

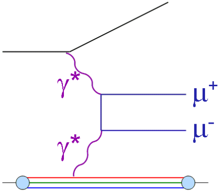

- J/ψ and $\psi(2S)$ mesons production with the dissociation of the proton

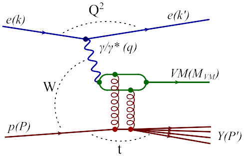

- Cosmic muons can mimic $\mu^+\mu^-$ pairs when passing close to the interaction point

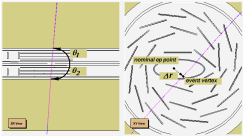

4-prongs: W and $|t|$ distributions: $\psi(2S)$ mass window

W: $3.4 < M(\mu^+\mu^-\pi^+\pi^-) < 4.0$ GeV

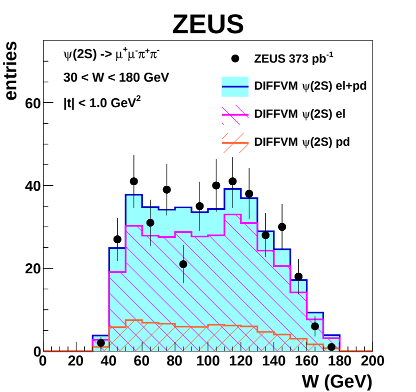

$|t|$: $3.4 < M(\mu^+\mu^-\pi^+\pi^-) < 4.0$ GeV

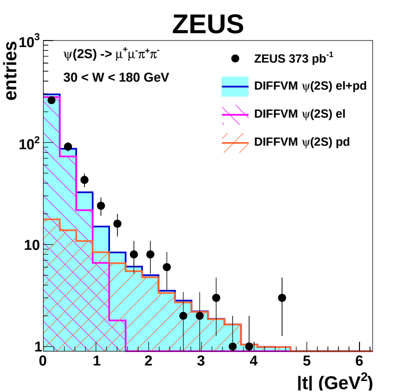

- proton dissociation dominates for $|t| > 1.0$ GeV^2
- proton dissociative fraction: $f_{p.diss} = 0.16 \pm 0.01$ ($|t| < 1.0$ GeV^2) from t-spectra fit

- **Monte Carlo**

DIFFVM – A Monte Carlo Generator for **Diffractive Processes in *ep* Scattering.**

B. List
CERN –EP/OPAL–,
CH–1211 Genève 23, Switzerland
Benno.List@cern.ch

A. Mastroberardino
Calabria University, Physics Dept.,
Cosenza, Italy
mastrobe@vxdesy.desy.de

- soft diffractive processes in the Regge framework and Vector Dominance Model
- $\frac{d\sigma}{dQ^2} \propto \frac{1}{(1+Q^2/M_V^2)^{1.5}}$
- $\frac{d\sigma}{d|t|} \propto W_{\gamma p}^{4\epsilon} e^{-b|t|}$ $(4\epsilon = \delta)$ (elastic)
- $\frac{d^2\sigma}{d|t|dM_Y^2} \propto W_{\gamma p}^{4\epsilon} e^{-b'|t|} M_Y^{-\beta}$ (p.diss)
- $\frac{d\sigma}{dM_Y^2} \sim \frac{f(M_Y^2)}{M_Y^{2(1+\epsilon)}}$ for $M_Y^2 < 3.6$ GeV^2 (p resonance region),
  $\frac{d\sigma}{dM_Y^2} \sim \frac{1}{M_Y^{2(1+\epsilon)}}$ for $M_Y^2 \geq 3.6$ GeV^2 (continuum region)
- assuming SCHC: s-channel helicity conservation

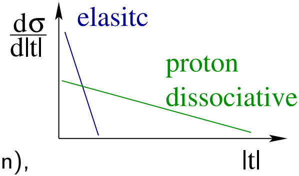

GRAPE-Dilepton
(Version 1.1)
A generator for dilepton production in *ep* collisions

Tetsuo Abe
Department of Physics, University of Tokyo, 7-3-1 Hongo, Bunkyo-ku, Tokyo 113-8654, Japan

- based on the exact matrix elements in the electroweak theory at tree level via $\gamma\gamma$, γZ^0, $Z^0 Z^0$
  and via photon internal conversion (QED Compton)
- Feynman amplitudes are generated by the automatic calculation system GRACE
- **proton vertex** covers the whole kinematical region
- interface to PYTHIA and SOPHIA
  $\rightarrow$ complete hadronic final state
- **covers elastic, quasi-elastic and DIS processes**

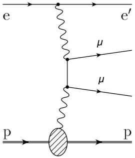

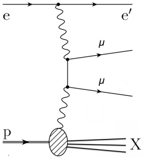

GRAPE generator - simulate QED lepton pair (Bethe-Heitler)

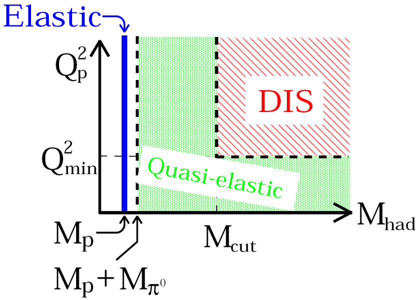

Important for the shape of the BH $M_{\mu^+\mu^-}$ spectrum (sidebands)
and for the BH t-dependence: low t - elastic BH, higher t - QEL BH

- **Tuning of** DIFFVM **Monte Carlo**

Tuning of DiffVM MC sample

- Reweighting of MC sample at generator level
- $|t|$ dependence: $\sim \exp(-b|t|)$, generated with $b_{el} = 4.0$, $b_{pd} = 1.0$
  reweighted to:
  $b_{el} = 4.6 \pm 0.3$, $b_{pd} = 1.0 \pm 0.1$ (JPSI)
  $b_{el} = 4.3 \pm 0.7$, $b_{pd} = 0.7 \pm 0.2$ (PSI2S)
- shrinkage added by reweighting: $b = b_0 + 4.0\alpha' \log(W/W_0)$;
  $\alpha' = 0.12 \pm 0.04$ GeV^{-2}, $W_0 = 90$ GeV (elastic only)
- W dependence: $\sigma \sim W^{\delta}$,
  generated with $\delta = 0.88$ for both elastic and p.diss
  reweighted to:
  $\delta_{el} = 0.67 \pm 0.10$, $\delta_{pd} = 0.42 \pm 0.15$ (JPSI)
  $\delta_{el} = 1.10 \pm 0.20$, $\delta_{pd} = 0.70 \pm 0.30$ (PSI2S)
- M_Y dependence: $\sim \frac{1}{M_Y^{\beta}}$, generated with $\beta = 2.5$
  reweighted to $\beta = 2.4 \pm 0.3$ (both JPSI and PSI2S, p.diss only)
- **all parameters are subject to systematics checks**

- **selection efficiency**

Acceptance*efficiency in W bins: elastic

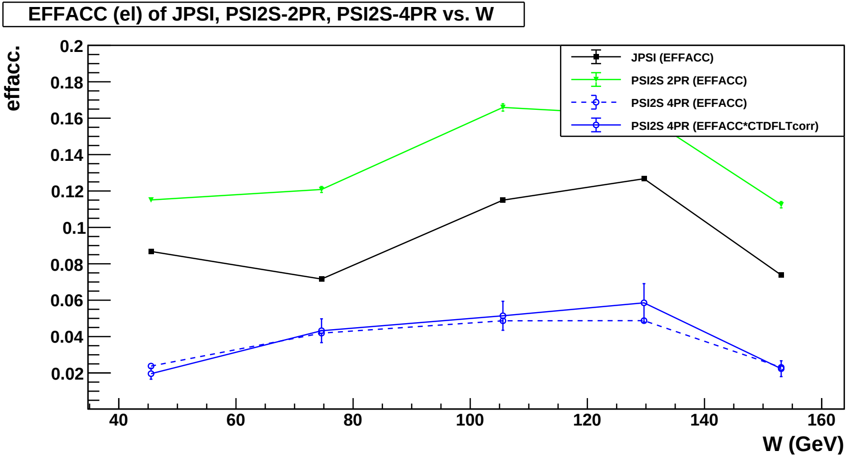

- JPSI, PSI2S 2- and 4-prong (**2 ÷ 16%**)
- Higher di-muon acceptance for higher mass state (PSI2S)
- different angular coverage for final state muons
- second W bin (W2) is the "dip" for di-muon acceptance

Acceptance*efficiency in $|t|$ bins: elastic

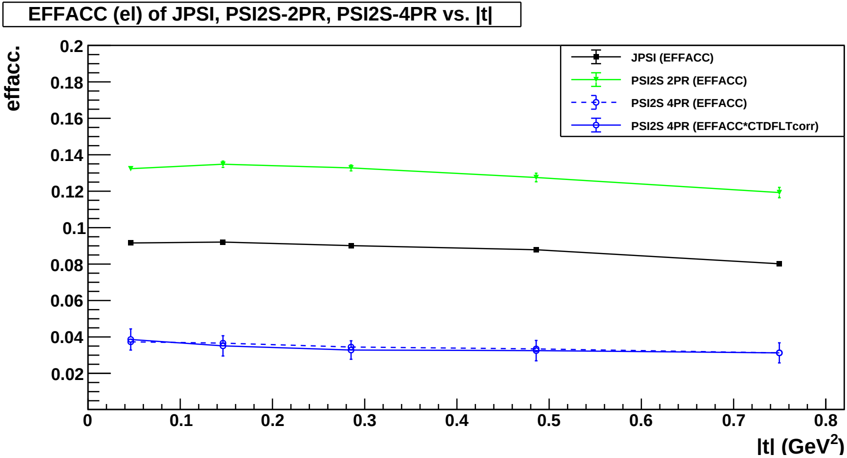

- JPSI, PSI2S 2- and 4-prong (**4 ÷ 12%**)
- Higher di-muon acceptance for higher mass state (PSI2S)
- flat in $|t|$ (no angular correlations to $|t|$)
- dashed line after CTD FLT corrections

p.diss fractions

- **extracting fractions of proton dissociation**

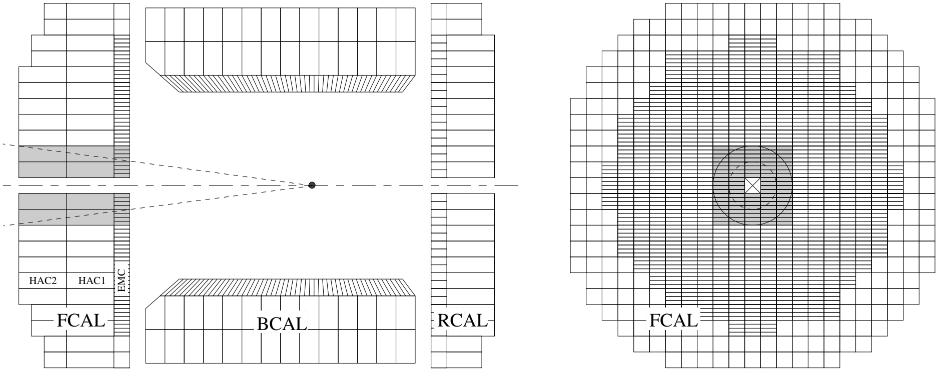

- Energy in forward cone to suppress p.diss events: $\theta_{max} = 0.12\,rad$
- using EFO : "Energy Flow Objects" (trackers + CAL info):

$$\left(\sum_{EFOs} E(\theta_{EFO} < \theta_{max})\right) < 1\,\mathrm{GeV}$$

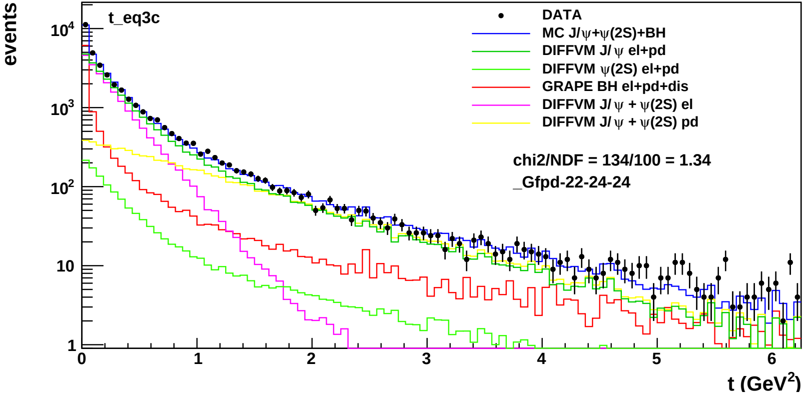

- **spectra like this are** used to evaluate the p.diss fractions (use longer "lever arm" then integrate it up to $|t| = 1.0$ GeV^2)
- using root package `TFractionalFitter` (TFF)
- fitted $f_{p.diss} = 0.17$ and $= 0.16$ (JPSI and PSI2S, BH subtracted)
- **p.diss take over elastic around $\sim$ 1 GeV^2** (yellow and magenta histos)

$f_{p.diss}$ fractions in W bins (TFF estimator)

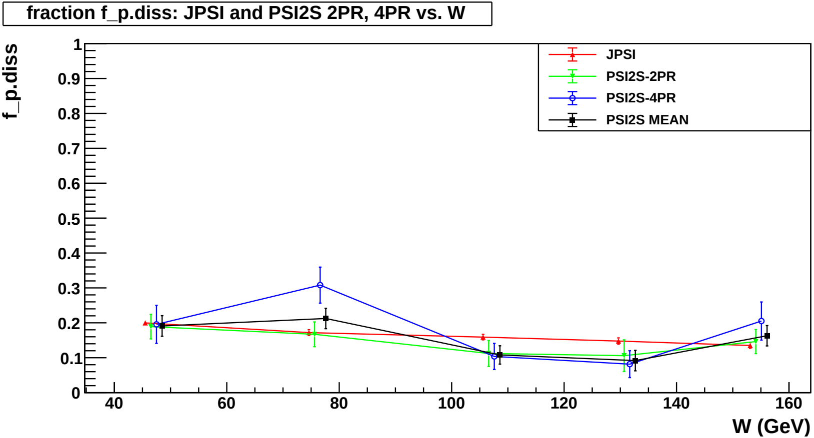

- average value $\sim$ 17% JPSI and $\sim$ 16% PSI2S (mean)
- compatible results for 2- and 4-prong channels, no W dependence
- **black**: weighted mean for PSI2S 2- and 4-prong
- bigger fluctuations for PSI2S 2- and 4-prongs

$f_{p.diss}$ fractions in W bins (TFF estimator)

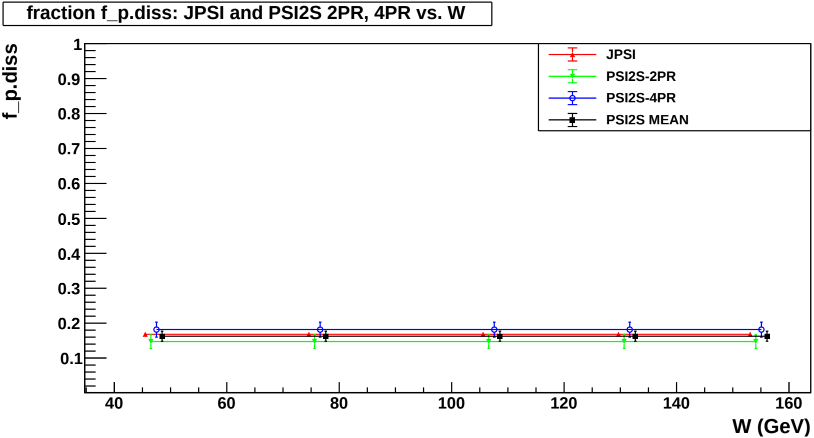

- average value $\sim 17\%$ JPSI and $\sim 16\%$ PSI2S (mean)
- **black**: weighted mean for PSI2S 2- and 4-prong (used in analysis)
- for R analysis: the same mean value is used for all W bins
- no significant impact on final ratio R ($f_{p.diss}$ fractions cancels out)

$f_{p.diss}$ fractions in $|t|$ bins (TFF estimator)

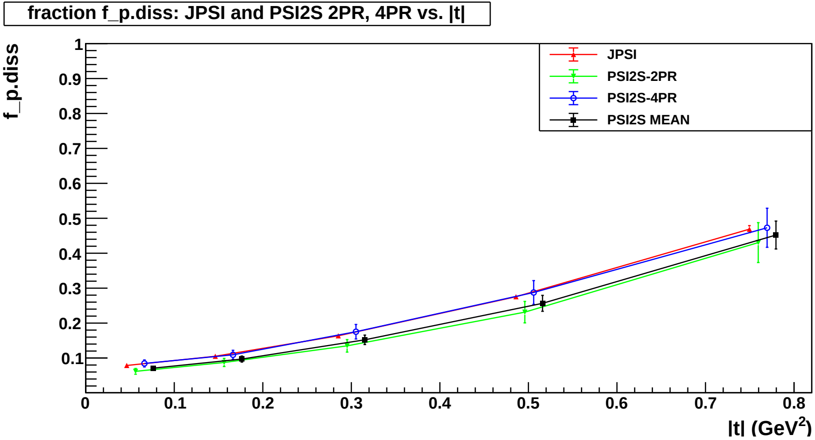

- compatible results for 2- and 4-prong channels
- **black**: weighted mean for PSI2S 2- and 4-prong (used in analysis)
- negligible effect on final R analysis ($f_{p.diss}$ fractions cancels out)
- bigger impact on systematics for large $|t|$ due to the b-slope variation !

- **Modeling of nucleon resonance states**
- (low M_Y proton dissociation)

Modeling of nucleon resonance state: DIFFVM

- $\frac{d\sigma}{dM_Y^2} \sim \frac{1}{M_Y^{2(1+\epsilon)}}$ for $M_Y^2 \geq 3.6\ \text{GeV}^2$ (continuum region)
- $\frac{d\sigma}{dM_Y^2} \sim \frac{f(M_Y^2)}{M_Y^{2(1+\epsilon)}}$ for $M_Y^2 < 3.6\ \text{GeV}^2$ (p resonance region)
- $f(M_Y^2)$ from the **fit the the p.diss cross section on deuterium**: $pD \to YD$ (Phys. Rep. **101** (3) (1983), 169)
- for $M_Y < 1.9$ GeV several resonances are included (Pomeron carries quantum numbers of the vacuum (I=0, G = P = C= +) only N^{*+} states with $J^{\mathcal{P}} = \frac{1}{2}^+, \frac{3}{2}^-, \frac{5}{2}^-, ...$)
- $N^{*+} = N(1440), N(1520), N(1680), N(1700)$
- N^{*+} decays into: $N\pi, \Delta\pi, N\rho, N\pi\pi$ included (BR from PGD 1992)
- N^{*+} decays isotropically in their rest frame

- dissociation in the continuum state carried by JETSET (splitting proton into $q - qq$ system, q couples to $\mathbb{P}$, leaving qq spectator)

- $d\sigma \sim L_{\mu\nu} W^{\mu\nu}$
- hadron tensor:

$$W^{\mu\nu} = W_1 \left(-g^{\mu\nu} + \frac{q^\mu q^\nu}{q^2} \right) + W_2 \frac{1}{M_P^2} \left(p_P^\mu - \frac{p_P \cdot q}{q^2} q^\mu \right) \left(p_P^\nu - \frac{p_P \cdot q}{q^2} q^\nu \right)$$

- $W_{1,2}(Q_P^2, M_{had})$ are proton electromagnetic structure functions
- for $M_{had} < 2$ GeV $W_{1,2}$ parameterized by Brasse at al. (Nucl. Phys. **B 110** (1976) 413.) (resonance region)
- for $M_{had} > 2$ GeV $W_{1,2}$ parameterized by ALLM97 (hep-ph/9712415) (continuum)
- both parameterizations from **fits to experimental total $\gamma^* p$ cross sections**
- exclusive hadronic final state generated by SOPHIA
- (plus DIS di-leptons diagrams, in the framework of QPM, using PDF's)

MC generator level: M_Y before and after selection cuts

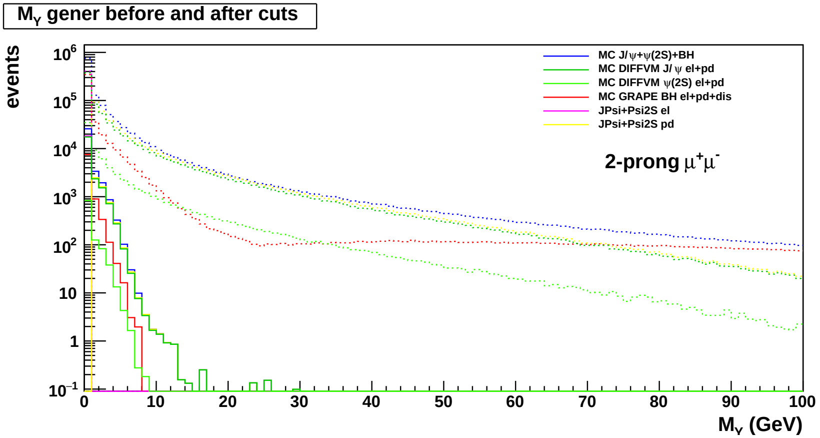

- M_Y at generator level (not measured quantity ! $\to$ lost in beam-pipe)
- before and after selection cuts
- GRAPE (BH) does include DIS scattering $\to$ rise of xsec. for large M_Y
- DIFFVM in DIS mode generates only **electroproduction** (with proton dissociation, "rapidity gap events") $\to$ this is OK

MC generator level: zoom at low $M_Y < 5$ GeV (lin scale)

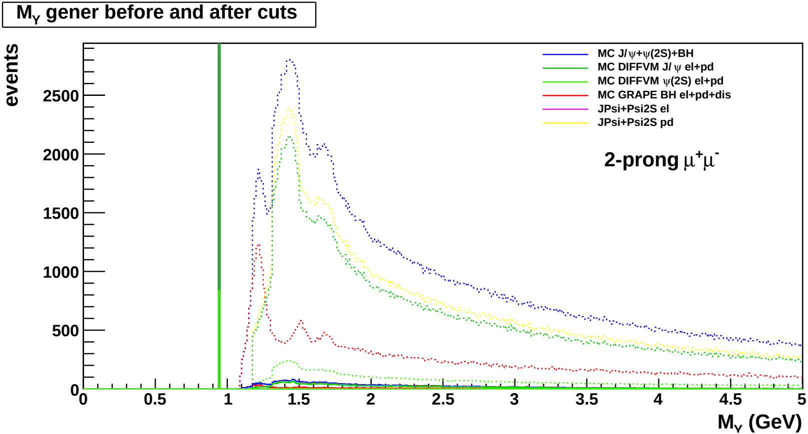

- different structure of nucleon resonances between GRAPE and DIFFVM (!?)
- which is right ?
- **how much it is important for p.diss BG subtraction ?**

- **Pions phase space reweighting**

- *weight* $= (M(\pi^-, \pi^+)^2 - 4.0 * M_\pi^2)^2$
- ref: `Phys_Lett_B61_1976_183.pdf`
- final $\pi^+\pi^-$ interaction is not in pure S-state
- $\rightarrow$ for the impact of this correction see next 2 pages

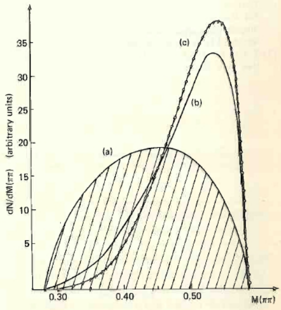

Fig. 4. Invariant mass distribution of two pions in S-state
Curve a $dN/dm_{\pi\pi} \propto$ phase space,
Curve b $dN/dm_{\pi\pi} \propto$ phase space $\times (s - 2\mu^2)^2$,
Curve c $dN/dm_{\pi\pi} \propto$ phase space $\times (s - 4\mu^2)^2$.

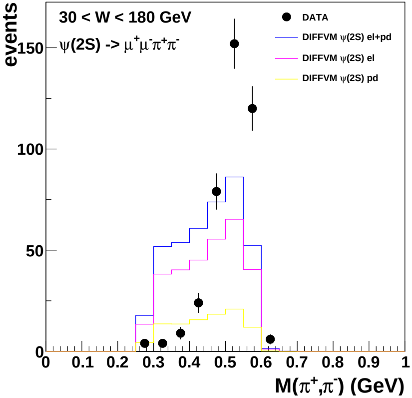

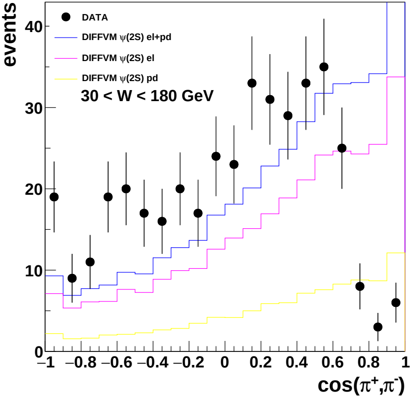

- $\psi' \to J/\psi + \pi^+\pi^-$
- $M(\pi^-,\pi^+)$, $\cos(\pi^-,\pi^+)$
- DIFFVM MC before pions phase space reweighting

4-PRONGS: $M(\pi^-, \pi^+)$, $\cos(\pi^-, \pi^+)$

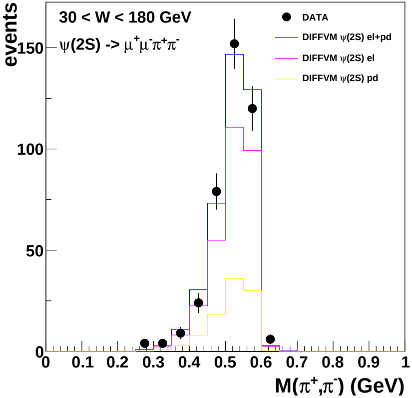

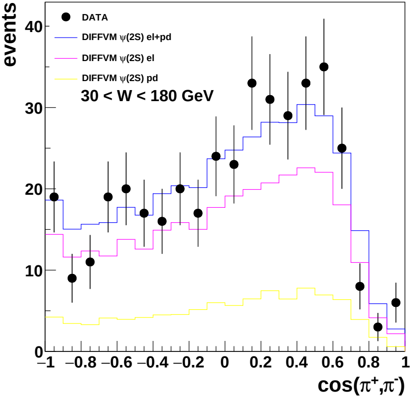

- $\psi' \to J/\psi + \pi^+\pi^-$
- $M(\pi^-, \pi^+)$, $\cos(\pi^-, \pi^+)$
- DIFFVM MC after pions phase space reweighting

Muon effic. corrections

- **Muon effic. corrections**

Muon effic. corrections: TAG and PROBE

- TAG: "the triggering" muon
- PROBE: "the tested" muon
- effic in given (pt^j_{eff}, η^j) bin: $\epsilon = N^j_{PROBE} / N^i_{TAG}$

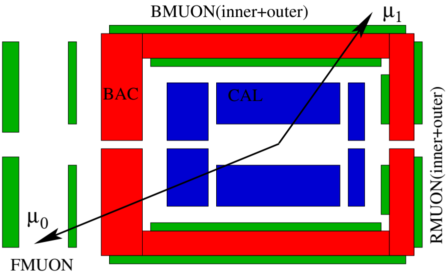

- one step correction for (FLT and SLT and TLT and off-line REC)
- separate maps for F/B/R/MUO, BAC and CAL (off-line only)
- evaluated for single muon in (pt_{eff}, η) bins, where as pt_{eff} is used:
  (motivated by the CAL/BAC geometry and scaling of the muon path length)
  - p in Forecap
  - p_t in Barrel
  - p_z in Rearcap
- proper identification of **the triggering muon** is crucial
- $\rightarrow$ the DATA/MC ratio delivers the correction weight: $\epsilon_x = \frac{\epsilon_{DATA}}{\epsilon_{MC}}$

Muon correction maps: $(p_z, p_t, p\ vs.\ \eta)$ - DATA

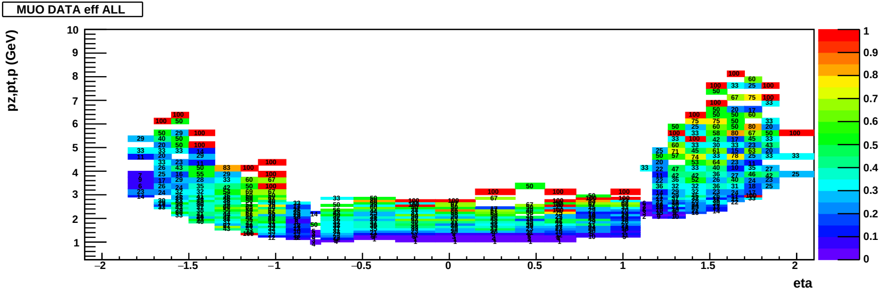

- **muon tomography**
- probability (%) to fire FLT-SLT-TLT-REC chain by single muon on $(p_z, p_t, p; \eta)$ grid
- X-axis (along eta): Rear-MUO, Barrel-MUO, Forward-MUO detectors
- only events with $M(\mu^+, \mu^-) < 6$ GeV
  (ie. in the phase space range of di-muon mass fits)
- current choice for p_z, p_t, p grid: 100 MeV per bin ($p_{eff} < 3$ GeV), 250 MeV per bin ($p_{eff} > 3$ GeV)
- size of the grid is subject to systematics